

Investigating Binary Black Hole Mergers with Principal Component Analysis

J. Clark¹, L. Cadonati^{1,2}, J. Healy⁴, I.S. Heng³, J. Logue³, N. Mangini¹, L. London⁴, L. Pekowsky⁴, D. Shoemaker⁴

Abstract Despite recent progress in numerical simulations of the coalescence of binary black hole systems, highly asymmetric spinning systems and the construction of accurate physical templates remain challenging and computationally expensive. We explore the feasibility of a prompt and robust test of whether the signals exhibit evidence for generic features that can educate new simulations. We form catalogs of numerical relativity waveforms with distinct physical effects and compute the relative probability that a gravitational wave signal belongs to each catalog. We introduce an algorithm designed to perform this task for coalescence signals using principal component analysis of waveform catalogs and Bayesian model selection and demonstrate its effectiveness.

1 Introduction

The coalescence of two black holes is arguably the most powerful source of gravitational waves (GWs) detectable by the second generation of ground based detectors: Advanced LIGO (Harry, 2010), Advanced Virgo (Acernese et al., 2009), and KAGRA (Somiya, 2012). The discovery of these signatures, forecast within the next few years (Aasi et al., 2013b), will open a new era of gravitational wave astrophysics, where the GW signature will provide insights on the physics of the source.

To decode the information in the GW waveform, we need a careful mapping with the masses and the spin magnitude and orientation of the black holes; this is the charge of numerical relativity (NR). While available NR waveforms span an increasing portion of the physical parameter space of unequal mass, spin and precessing binary black holes (BBHs) (Ajith et al., 2012; Hinder et al., 2014), each

¹ University of Massachusetts Amherst, Amherst, MA 01003, USA

² Cardiff University, Cardiff, CF24 3AA, United Kingdom

³ SUPA, School of Physics and Astronomy, University of Glasgow, G12 8QQ, United Kingdom

⁴ Center for Relativistic Astrophysics, Georgia Institute of Technology, Atlanta GA 30332

simulation takes a week or more to run. A complete coverage of the full parameter space remains a slow but important endeavor to enable GW matched filtering and parameter estimation (Thorne, 1987; Aasi et al., 2013a).

The LIGO and Virgo Collaborations have refined techniques for the search of generic GW transients, or *bursts*, which don't assume a specific waveform but rely on a coherent GW in multiple detectors for a variety of plausible sources (Abadie et al., 2012; Andersson et al., 2013). The work presented here aims to answer the question of how a transient detected by a template-less burst search can trigger new NR simulations in interesting regions of the BBH parameter space. We introduce a proof-of-concept study, which uses the method of Principal Component Analysis (PCA) to compare a plausible signal to catalogs of NR waveforms, which represent certain regions of the BBH physical parameter space.

2 Binary Black Hole Merger Simulations

The GW waveform produced by solar and intermediate mass BBH systems spans the sensitive band of ground based detectors through the inspiral, merger and ringdown phases. While post-Newtonian and perturbation theories adequately describe the inspiral and ringdown, numerical relativity is necessary to capture the physics of the merger. NR has been probing the parameter space of binary black hole mergers since the breakthrough of 2005 (Pretorius, 2005) achieving extreme mass ratios (Lousto and Zlochower, 2011), extreme spin magnitudes (Lovelace et al., 2012) and many precessing runs (Mroue et al., 2013; Pekowsky et al., 2013).

The NR waveforms used in this paper were produced by the MAYA code of the Georgia Institute of Technology (Vaishnav et al., 2007). The MAYA code uses the Einstein Toolkit¹, which is based on the CACTUS² infrastructure and CARPET mesh refinement (Schnetter et al., 2004). The output of all simulations is the Weyl Scalar, Ψ_4 , decomposed into spin-weighted spherical harmonics that is then converted to strain (Reisswig and Pollney, 2011).

For this work we use 48 NR runs, listed in Table 1 without hybridization with post-Newtonian waveforms. The Q-series contains 13 non-spinning, unequal-mass

Table 1 Physical parameters for the three catalogs used in this study.

Name	Q	HR	RO3
Mass Ratio, $q = m_1/m_2$	1 – 2.5	1 – 4	1.5 – 4
Spin magnitude, a	0.0	0.0 – 0.9	0.4, 0.6
Tilt Angle, θ	0.0	0.0	$45^\circ - 270^\circ$
N waveforms	13	15	20

¹ <http://www.einsteintoolkit.org>

² <http://www.cactuscode.org>

simulations. We use 15 runs from the HR-series, a set of unequal-mass, equal spin simulations, with initial spin parallel to the initial angular momentum. The RO3-series is a set of 20 unequal-mass simulations with the lighter black hole spin aligned to the initial angular momentum (z-axis) and the other black hole at a tilt angle θ with the z-axis in the xz-plane; these systems are precessing and the tilt-angles are defined at a specific separation of the black holes at one instant in the evolution of the binary system and change in time. While the runs are tabulated with initial parameters, there is no functional form to relate one waveform to the next; we use a Principal Component Analysis to determine the main features of each catalog.

3 Principal Component Analysis and Bayesian Model Selection

We parametrize the NR waveform catalogs of §2 with an orthonormal set of principal components (PCs), obtained with a standard singular value decomposition (Heng, 2009; Röver et al., 2009). For a catalog of n waveforms $\{h_i\}_{i=1,\dots,n}$ with m samples, we create a matrix \mathbf{H} whose columns corresponds to each waveform. We then factorize the resulting $m \times n$ matrix \mathbf{H} so that:

$$\mathbf{H} = \mathbf{U}\mathbf{S}\mathbf{V}^T, \quad (1)$$

where \mathbf{U} is an $m \times m$ matrix whose columns are the eigenvectors of $\mathbf{H}\mathbf{H}^T$ and \mathbf{V} is an $n \times n$ matrix whose columns are eigenvectors of $\mathbf{H}^T\mathbf{H}$. The $m \times n$ matrix \mathbf{S} will have all zeros, except for the $\{S_{jj}\}_{j=1,\dots,n}$ terms, which correspond to the square root of the j th eigenvalue. \mathbf{U} contains the catalog's PCs, ranked by their corresponding eigenvalue: the first column is the first PC, which encapsulates the most significant features common to all waveforms in the catalog, the second column, corresponding to the second largest eigenvalue, describes the second most significant common features in the catalog, and so on. The waveforms in \mathbf{H} can be reconstructed as a linear combination of PCs:

$$h_i \approx \sum_{j=1}^k U_j \beta_j, \quad (2)$$

where h_i is the catalog waveform, u_j is the j th PC and β_j is the corresponding coefficient, obtained by projecting h_i onto u_j . The sum over k PCs is an approximation of the desired waveform, since in general $k < n$. In this analysis, the choice of k is determined by the *cumulative eigenvalue energy*, $E(k)$, shown in Figure 1:

$$E(k) = \frac{\sum_{i=1}^k S_{ii}}{\sum_{j=1}^n S_{jj}} \quad (3)$$

In this analysis we use k PCs, so that $E(k) \geq 0.9$. This corresponds to 2, 4 and 5 PCs for the Q, HR and RO3 catalogs respectively. A selection of the waveforms from the HR catalog and corresponding PCs are shown in Figure 2.

Fig. 1 Cumulative eigenvector energy as a function of the number of principal components for the three catalogs in this study. We use the number of PCs that provides 90% of the energy: 2 PCs for set Q, 4 PCs for set HR and 5 PCs for set RO3.

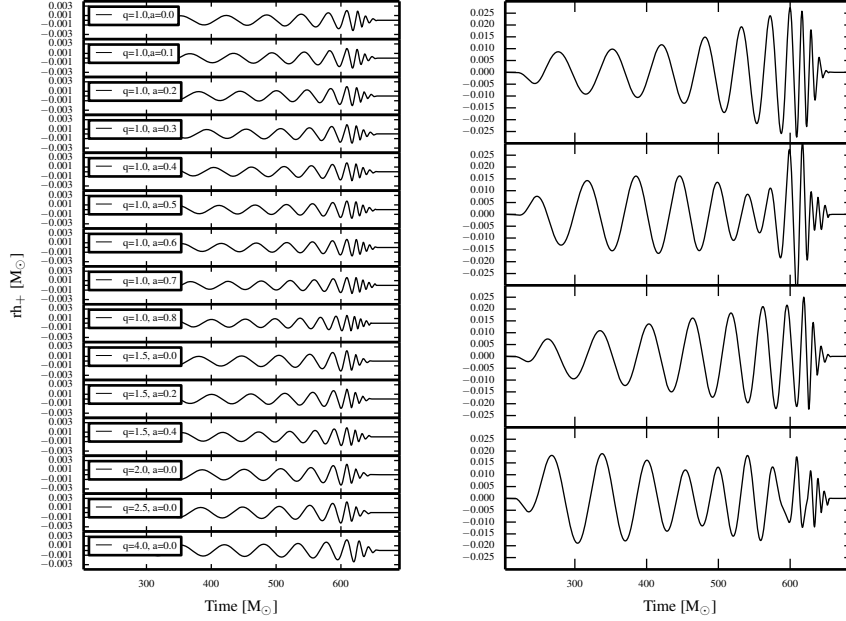
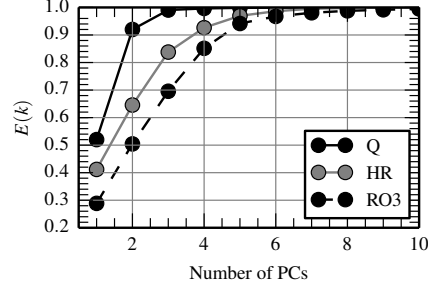


Fig. 2 *Left*: the waveforms in the HR catalog of spinning, non precessing waveforms used in this study. *Right*: The principle component decomposition of the HR catalog.

Following the seminal work on Burst signals in (Clark et al., 2007; Logue et al., 2012), the PCs can be used to identify generic features for a measured waveform through the posterior odds ratio, which is widely used in GW data analysis to compare the probabilities of two competing models M_i and M_j . Given data D , the odds ratio \mathcal{O}_{ij} is the ratio of posterior probabilities for each model:

$$\mathcal{O}_{ij} = \frac{p(M_i)}{p(M_j)} \frac{p(D|M_i)}{p(D|M_j)} = \pi_{ij} \frac{Z_i}{Z_j}, \quad (4)$$

where π_{ij} is the *prior odds ratio* which reflects any bias one has for the models. Z_i is the evidence for model M_i . The evidence ratio Z_i/Z_j is referred to as the Bayes'

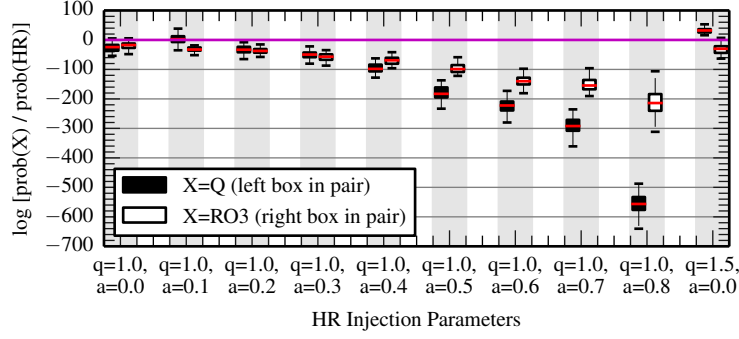


Fig. 3 Distribution of Bayes factors for HR waveforms. Each pair of boxes in the figure corresponds to the sample of Bayes factors (equation 5) for the 50 different noise realizations. The boxes denote the interquartile range of the distribution, the red lines indicate the median value and the whiskers show the outliers within $1.5\times$ the interquartile range. The x -axis indicates the physical parameters of the injection performed; for the HR catalog, the mass ratio and spin magnitudes are varied. The two $a = 0$ systems are seen to be difficult to distinguish from the Q catalog which is not surprising since Q catalog contain waveforms for non-spinning systems.

factor B_{ij} and reflects the influence of the data. To demonstrate the efficiency of our algorithm, we assume here $\pi_{ij} = 1$. In this context, the models are the waveform catalogs and the evidences are obtained by marginalizing over all model parameters which are the $\{\beta_j\}$ coefficients used to construct the signal model in equation 2 from the catalog's PCs. We adopt a uniform prior for $\{\beta_j\}$, in a range obtained by projecting the waveforms from each catalog onto its corresponding PCs. As in (Logue et al., 2012), the likelihood and corresponding evidences are computed with a nested sampling algorithm. The model evidence is largest for the most parsimonious model that best explains the data; $B_{ij} > 1$ indicates M_i is preferred over M_j .

4 Identifying Binary Black Hole Merger Phenomenology

We demonstrate the efficacy of the PCA-based Bayesian model selection with a Monte-Carlo analysis where simulated GW signals from each catalog are added to colored, Gaussian noise, which is generated as in Logue et al. (2012). For this proof-of-principle study we assume a single aLIGO detector operating at design sensitivity in the “zero-detuned, high-power” configuration (Harry, 2010). We make the further assumptions that the time of peak amplitude of the signal is known, that the source is optimally oriented and located on the sky with respect to the detector and, finally, that the total mass of the system is $250M_\odot$. This choice of mass ensures that the signals “switch on” below the minimum sensitive frequency of the aLIGO noise spectrum (10 Hz). The physical distance of the simulated signal is scaled such that the injections have SNR=50. The GW signals from our catalogs are injected into

50 independent noise realizations. Thus, for each waveform we obtain 50 evidence values for the waveform to belong to one of the catalogs: Z_Q , Z_{HR} and Z_{RO3} .

To demonstrate that model selection can correctly identifying which catalog a given injection originated from, for an injection from a given catalog C we form the Bayes factors between the other catalogs and the model M_C . For example, if an injection is performed from the HR catalog, we compute the log Bayes factors:

$$\log B_{Q,HR} = \log Z_Q - \log Z_{HR} \quad \text{and} \quad \log_e B_{RO3,HR} = \log Z_{RO3} - \log Z_{HR} . \quad (5)$$

If the algorithm correctly discriminates between the waveform catalogs, both $B_{Q,HR}$ and $B_{RO3,HR}$ will be less than unity.

Figure 3 summarizes the distribution of Bayes factors for HR waveforms. The majority of the boxes lie well below zero, indicating that the algorithm correctly identifies the HR catalog as the most probable for these simulations, with $Z_{HR} > \max(Z_Q, Z_{RO3})$. Qualitatively similar results are found when analyzing signals from the Q and RO3 catalogs and will be explored more fully in a follow-up publication.

Acknowledgements This work was supported by NSF grants PHY-0955773 and 0955825, SUPA and STFC UK. Simulations were supported by NSF XSEDE PHY120016 and PHY090030, and CRA Cygnus cluster.

References

- J. Aasi, et al. Phys. Rev. D **88**, 062001 (2013a)
- J. Aasi, et al., 2013b. Preprint arXiv:1304.0670
- J. Abadie, et al. Phys. Rev. D **85**, 122007 (2012)
- F. Acernese, et al., 2009. <https://tds.ego-gw.it/ql/?c=6589>
- P. Ajith, et al. Class. Quant. Grav. **29**, 124001 (2012)
- N. Andersson, et al. Class. Quant. Grav. **30**, 193002 (2013)
- J. Clark, et al. Phys. Rev. D **76**, 043003 (2007)
- G.M. Harry Class. Quant. Grav. **27**, 084006 (2010)
- I.S. Heng Class. Quant. Grav. **26**, 105005 (2009)
- I. Hinder, et al. Class. Quant. Grav. **31**, 025012 (2014)
- J. Logue, et al. Phys. Rev. D **86**, 044023 (2012)
- C.O. Lousto, Y. Zlochower Phys. Rev. Lett. **106**, 041101 (2011)
- G. Lovelace, et al. Class. Quant. Grav. **29**, 045003 (2012)
- A.H. Mroue, et al. Phys. Rev. Lett. **111**, 241104 (2013)
- L. Pekowsky, et al. Phys. Rev. D **88**(2), 024040 (2013)
- F. Pretorius Phys. Rev. Lett. **95**, 121101 (2005)
- C. Reisswig, D. Pollney Class. Quant. Grav. **28**, 195015 (2011)
- C. Röver, et al. Phys. Rev. D **80**, 102004 (2009)
- E. Schnetter, et al. Class. Quant. Grav. **21**, 1465–1488 (2004)
- K. Somiya Class. Quant. Grav. **29**, 124007 (2012)
- K.S. Thorne, in *300 Years of Gravitation*, ed. by S.W. Hawking, I. W. (Cambridge University Press, Cambridge, UK, 1987)
- B. Vaishnav, et al. Phys. Rev. D **76**, 084020 (2007)